OPEN ACCESS

REGULAR ARTICLE

Study of Effect of Temperature on Lead Free Cesium-Based Double Perovskite Solar Cell by Using SCAPS-1D

S. Das, S. Narzary, K. Chakraborty, S. Paul

Advanced Materials Research and Energy Application Laboratory (AMREAL), Department of Energy Engineering, North-Eastern Hill University, Shillong-793022, India

The pernicious and stability concerns of lead based perovskite solar cells have limited the commercialization. The lead-free Cesium based double perovskite could be a viable answer to these issues. It exhibits encouraging optoelectronic properties, high environmental stability and low toxicity. In this present work a theoretical analysis of Cesium based double perovskite solar cell using Spiro-OMeTAD as hole transport layer and SnO2 as ETL has been studied. The double perovskite $Cs_2AgBiBr_6$ has good optical and electronic features. For this study, a device structure of FTO/SnO₂/Cs₂AgBiBr₆/Spiro-OMeTAD/Cu was simulated. The Solar Cell Capacitance Simulator (SCAPS-1D) was used for one dimensional simulation and analysis. The optimized active layer of 0.3 μm was used for the study. PCE, V_{oc}, J_{sc} and FF were obtained using Spiro-OMeTAD as HTL and SnO₂ as ETL. The maximum PCE of 10.6675% and the maximum quantum efficiency of 86.17025% were found at 275 K working temperature. The simulation results obtained in this study are encouraging. It will provide insightful guidance in replacing commonly used toxic Pb-based perovskite with eco-friendly, highly efficient inorganic double perovskite solar cell.

Keywords: SCAPS-1D, Double perovskite, Photovoltaic, ETL, HTL, QE, PCE, FF.

1. INTRODUCTION

The incessant utilization of fossil fuels has drawn attention to alternative energy resources. Out of many available renewable energy sources, solar energy is the most promising and widely preferred [1-5]. In the recent past, organic-inorganic metal halide perovskite solar cells have been explored as an alternative to silicon-based solar cells for improving efficiency and are also preferred because of low manufacturing cost [6-10]. Lead (Pb) halide perovskites have excellent optoelectronic properties but the toxicity of Pb and poor stability are the principal reasons for not being suitable for commercial applications [11-16]. Lead-free double perovskites such as Cs2AgBiBr6 have attractive optical and electronic properties. In this work, we have considered fully inorganic Cs2AgBiBr6 as the absorber layer in the lead-free double perovskite solar cell (DPSC) n-i-p structure. Spiro-OMeTAD was employed as the hole transport layer. Fluorine-doped tin oxide and copper were employed as the front and back contact respectively. The DPSC structure FTO/ SnO2/Cs2AgBiBr6/Spiro-OMeTAD/Cu was optimized by applying the various ETLs. The optimized thickness of the absorber layer, HTL and ETL were used. All these simulations were performed using SCAPS-1D. The main purpose of this present work is to find an efficient and lead-free double perovskite solar cell, by studying the effect of working temperature. The most suitable working temperature for the proposed device structure has been found without doing any experimental efforts which takes a lot of resources.

2. METHODOLOGY AND DEVICE ARCHITECTURE

The theoretical study of the device helps us in understanding the device mechanism without actual fabrication. It also gives an outline of the performance of the device. To study the solar cell device theoretically, we have used SCAPS-1D solar cell simulation program for the simulation of our device. This software was developed by University of Gent, Belgium in 2000 and is freely available now [16-19]. The SCAPS program facilitates the modeling of planar as well as graded device structures up to seven layers and it has also the capability of computing the band alignment diagram, current-voltage characteristics, quantum efficiency, recombination and generation currents and other important parameters of the device. The SCAPS-1D is a one dimensional solar cell simulation program based on three coupled differential equations, namely Poisson's equation, the continuity equation for the electrons and the continuity equation for holes as follows:

$$\frac{d}{dx}\left(-\varepsilon(x)\frac{d\Psi}{dx}\right) = q[p(x) - n(x) + N_d^+(x) - N_a^-(x) + p_t(x) - n_t(x)] \quad (1)$$

$$\frac{dp_n}{dt} = G_p - \frac{p_n - p_{n0}}{\tau_p} - p_n \mu_p \frac{d\xi}{dx} - \mu_p \xi \frac{dp_n}{dx} + D_p \frac{d^2 p_n}{dx^2} \quad (2)$$

$$\frac{dn_p}{dt} = G_n - \frac{n_p - n_{p0}}{\tau_n} + n_p \mu_n \frac{d\xi}{dx} + \mu_n \xi \frac{dn_p}{dx} + D_n \frac{d^2 n_p}{dx^2} \quad (3)$$

Here, D is diffusion coefficient, Ψ is electronic potential, q is electron charge, G is generation rate, ξ is permittivity, and n, p, n_t, and p_t are free holes, free electrons, trapped holes, and trapped electrons, respectively. N_a^- refers to ionized acceptor like doping concentration, and N_d^+ stands for ionized donor-like doping concentration.

In the present work, we have studied a conventional planar n-i-p device structure with lead free fully inorganic double perovskite $Cs_2AgBiBr_6$ as the absorber layer, Spiro-OMeTAD as the hole transport layer, different ETLs (SnO_2, TiO_2, ZnO-NR and CdS), fluorine doped tin oxide (FTO) and copper (Cu) as the front and back contacts respectively. The schematic of the device structure FTO/ETLs/$Cs_2AgBiBr_6$/Spiro-OMeTAD/Cu has been shown in Fig. 1.

Fig. 1 – Device Structure used for Simulation

The physical parameters of the material like bandgap (E_g), electron affinity (χ), dielectric permittivity (ε), conduction and valence band density of state (N_c and N_v), electron and hole thermal velocities (v_e and v_h), acceptor and donor density (N_A and N_D) and defect density (N_l) are employed as the input parameters for the device simulation. These all parameters have been taken from the theoretical and experimental reported works and are given in Table 1 and 2 [16-20].

Table 1 – SCAPS 1-D input material parameters [8-11]

Parameters	Window Layer (FTO)	HTL (Spiro-OMeTAD)	Absorber Layer ($Cs_2AgBiBr_6$)	ETL (SnO_2)
Thickness, μm	0.2	0.3	0.3	0.3
Bandgap (E_g), eV	3.2	3.0	2.05	3.6
Electron affinity (χ), eV	4.4	2.45	4.19	4.4
Relative Permittivity (ε_r)	9.0	3.0	5.80	9
CB effective density of states (N_c), cm^{-3}	2.2E+18	2.2E+19	1.0E+16	2.2E+18
VB effective density of states (N_v), cm^{-3}	1.8E+19	1.8E+19	1.0E+16	1.8E+19
Electron mobility (μ_n), cm^2·V^{-1}·s^{-1}	20	2.0E-4	11.81	100
Hole mobility (μ_p), cm^2·V^{-1}·s^{-1}	10	2.0E-4	0.49	2.56E-1
Donor density (N_d), cm^{-3}	1.0E+18	0	1.0E+19	1E+17
Acceptor density (N_a), cm^{-3}	0	1.0E+18	1.0E+19	0
Defect Density (N_l), cm^{-3}	1.0E+15	1.0E+14	9.1E+16	1E+15

3. RESULT AND DISCUSSION

In this work, we have used SnO_2 as the ETL layer for the simulation of DPSC. The energy band alignment diagram is shown in Fig. 2. This work focuses on to promote a lead free double perovskite solar cell structure with Spiro-OMeTAD as the HTL. Along with the J-V characteristics, effect of some fundamental parameters such as band gap, electron affinity, dielectric permittivity, electron affinity, dielectric permittivity, electron and hole mobility has also been observed using SnO_2 as the ETL. The optimum values of parameters are based on reported literatures [5-10] which are summarized in Table 1.
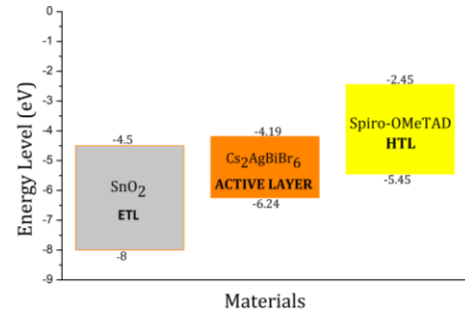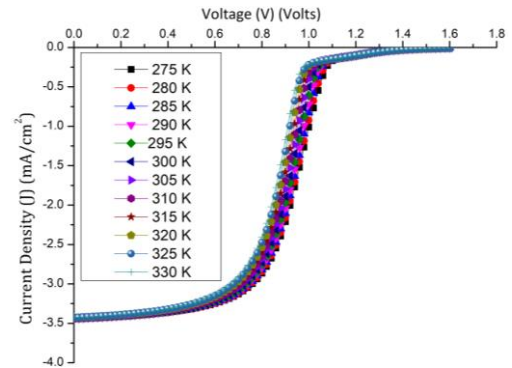

**Fig. 2** – Energy band alignment

Fig. 3 – *J-V* curves at different working temperatures

Study of Effect of Temperature on Lead Free Cesium-Based ...

J. NANO- ELECTRON. PHYS. **16**, 05009 (2024)

Table 2 – Working temperature effect on PCE

Working temperature (K)	J_{sc} (mA/cm²)	PCE (%)
275	3.44031	10.6675
280	3.43946	10.5921
285	3.43854	10.5145
290	3.43755	10.4281
295	3.43648	10.3318
300	3.43532	10.2362
305	3.43406	10.1363
310	3.4327	10.0245
315	3.43124	9.9085
320	3.42966	9.7918
325	3.42797	9.6614
330	3.42614	9.532

The working temperature has a significant impact on the photovoltaic device performance. The performance of photovoltaic cells was reduced as a result of the increased heating in a solar cell due to sunshine. We choose a temperature range of 275 to 330 K for our study. Fig. 3 shows the simulation result of *J-V* characteristic curves affected by the working temperature. The higher temperatures affect the material carrier concentration and band gaps. Also, the electron and hole motilities are affected by the increased temperature. As a result the efficiency of the solar cell decreases with rise in temperature. Saturation current in reverse J₀ is temperature dependent and as a result V$_{oc}$ drops as the temperature rises. As the temperature rises, the reverse saturation current decreases and this drop in current is the main source of the fall in V_{oc}, as can be inferred from Eq. 4 [17-20].

$$J_e(V) = J_0[exp(qV_{oc}/k_BT) - 1] \qquad (4)$$
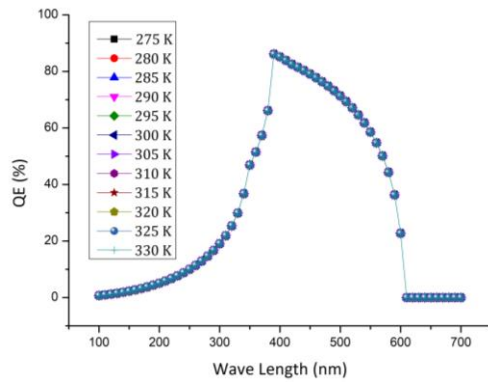
Fig. 4 – QE curves at different working temperatures

Table 3 – Working temperature effect on QE

Working temperature (K)	Maximum QE at 390 nm wavelength (%)
275	86.17025
280	86.16888
285	86.16668
290	86.16347
295	86.15952
300	86.1547
305	86.14913
310	86.14283
315	86.13548
320	86.12736
325	86.11875
330	86.10946

The greater working temperature provides more energy to electrons. These electrons are more likely to recombine with the holes before reaching the depletion area. The PCE of a cell diminishes as the temperature rises and the J_{sc} also decreases as shown in Fig. 3. From Fig. 4, we find the maximum quantum efficiency of 86.17025% was found at around 390 nm wavelengths and at 275 K working temperature. The Table 3 summarizes the maximum QE at 390 nm wavelength. It can clearly be observed from Table 2 that the DPSC has the best performance when the working temperature is 275 K. So the device can be used especially in cold regions.

4. CONCLUSION

For the justification of our proposed model, simulation has been done for lead free DPSC structure using SCAPS-1D. The simulations of lead-free double perovskite $Cs_2AgBiBr_6$ based solar cell having Spiro-OMeTAD as the hole transport layer and SnO_2 as the ETL material have been used. From the simulations, it has been deduced that *J-V* characteristics of the DPSC model have indicated high-efficiency performance. The best performance has been achieved for the lead free DPSC at 275 K (J_{sc} = 3.44031 mA/cm², PCE = 10.6675%, QE = 86.17025%). Simulations have been done to analyze the effects of electrical parameters on lead free double perovskite $Cs_2AgBiBr_6$ based solar cell. From the results of the simulations, it can be summarized that FTO/SnO_2/$Cs_2AgBiBr_6$/Spiro-OMeTAD/Cu lead free DPSC structure is a potential alternative for solar cell which can be reasonably efficient and inexpensive. Since the DPSC has the best performance when the working temperature is 275 K, therefore the device can be used especially in cold regions. For further improvement of performance, effects of the defect state of the interface defect layer, effect of density of state on the absorber layer and effect of different back contacts need to be studied. Experimental studies are also needed for extensive investigation regarding our proposed lead free double perovskite solar cell (DPSC) structure.

REFERENCES

1. S.A. Moiz, *Photonics* **9** No 1, 23 (2022).
2. S. Das, et al., *J. Nano- Electron. Phys.* **16** No 1, 01014 (2024).
3. A. Tara, et al., *Opt. Mater.* **119**, 111362 (2021).
4. I.I. Jeon, et al., *Nanomaterials* **11** No 8, 2066 (2021).
5. R. Mouchou, et al., *Mater. Today Proc.* **38** No 2, 835 (2021).
6. A.K. Das, et al., *Opt. Quant. Electron.* **54** No 7, 455 (2022).
7. Abdelaziz, et al., *Opt. Mater.* **123**, 111893 (2022).
8. H. Sabbah, *Materials* **15** No 9, 3229 (2022).
9. S. Das, et al., *J. Nano- Electron. Phys.* **14** No 3, 03012 (2022).
10. Y. Yan, et al., *ACS Appl. Mater. Interface.* **13** No 33, 39371 (2021).
11. N. Singh, et al., *Opt. Mater.* **114**, 110964 (2021).
12. S. Das, et al., *J. Nano- Electron. Phys.* **13** No 3, 03018 (2021).
13. F. Izadi, et al., *Optik* **227**, 166061 (2021).
14. A. Benzetta, et al. *Optik* **242**, 167320 (2021).
15. A. Sunny, et al., *AIP Adv.* **11**, 065102 (2021).
16. M.S. Salem, et al., *Energies* **14** No 18, 5741 (2021).
17. S.S. Hussain, et al., *J. Renew. Energy* **2021**, 6668687 (2021).
18. T. Ouslimane, et al., *Heliyon* **7** No 3, 06379 (2021).
19. M. Mottakin, et al., *Energies* **14** No 21, 7200 (2021).
20. K. Bhavsar, P. Lapsiwala, *Semiconductor Physics, Quantum Electronics & Optoelectronics* **24** No 3, 341 (2021).

Дослідження впливу температури на безсвинцевий подвійний перовскітний сонячний елемент на основі цезію за допомогою SCAPS-1D

S. Das, S. Narzary, K. Chakraborty, S. Paul

Advanced Materials Research and Energy Application Laboratory (AMREAL), Department of Energy Engineering, North-Eastern Hill University, Shillong-793022, India

Проблеми стабільності перовскітних сонячних батарей на основі свинцю обмежили комерціалізацію. Подвійний перовскіт на основі цезію, що не містить свинцю, може стати життєздатною відповіддю на ці проблеми. Він демонструє вражаючі оптоелектронні властивості, високу екологічну стабільність і низьку токсичність. У цій роботі було вивчено теоретичний аналіз подвійного перовскітного сонячного елемента на основі цезію з використанням Spiro-OMeTAD як шару транспортування дірок і SnO_2 як ETL. Подвійний перовскіт $Cs_2AgBiBr_6$ має хороші оптичні та електронні властивості. Для цього дослідження була змодельована структура пристрою $FTO/SnO_2/Cs_2AgBiBr_6/Spiro-OMeTAD/Cu$. Симулятор ємності сонячних батарей (SCAPS-1D) використовувався для одновимірного моделювання та аналізу. Для дослідження використовувався оптимізований активний шар 0,3 мкм. PCE, V_{oc}, J_{sc} і FF були отримані з використанням Spiro-OMeTAD як HTL і SnO_2 як ETL. Максимальний PCE 10,6675% і максимальна квантова ефективність 86,17025% були знайдені при робочій температурі 275 K. Результати моделювання, отримані в цьому дослідженні, є обнадійливими. Він надасть глибокі вказівки щодо заміни зазвичай використовуваного токсичного перовскіту на основі Pb екологічно чистими, високоефективними неорганічними подвійними перовскітними сонячними елементами.

Ключові слова: SCAPS-1D, Подвійний перовскіт, Фотоелектричні властивості, ETL, HTL, QE, PCE, FF.